Spectral Gain Narrowing in THz quantum cascade lasers

S. Dhillon,[a] N. Jukam,[a] D. Oustinov,[a] Z. Y. Zhao,[a] S. Hameau,[a] S. Barbieri,[b] A. Vasanelli,[b] P. Filloux,[b] X. Marcadet,[c] C. Sirtori,[b] J. Tignon[a]

[a] Laboratory Pierre Aigrain, Ecole Normale Supérieure, 24 rue Lhomond, 75005 Paris, France

[b] Matériaux et Phénomènes Quantiques, University Paris VII, 10 rue A. Domont et L. Duquet, 75013 Paris, France

[c] Thales Research and Technology, Route Départementale 128, 91767 Palaiseau cedex, France

Abstract - Terahertz time-domain spectroscopy is used to determine gain related parameters of terahertz quantum-cascade lasers. Due to the techniques' insensitivity to the QCL emission, spectral gain narrowing is observed above laser threshold. By correlating these measurements with bandstructure simulations, insight into the subband alignment as a function of the applied field is acquired.

I. Introduction And Background

Terahertz (THz) quantum cascade lasers (QCLs) are one of the few semiconductor based laser sources operating in the THz range. Since their realisation in 2002,[1] they have showed considerable advances such as extension to low frequencies, sub-wavelength dimensions and above liquid nitrogen temperature operation.[2] Even with these advancements, however, there is a considerable lack of information on the internal mechanisms of such complex devices. In this work THz time domain spectroscopy (TDS) is used to investigate key parameters such as the spectral gain and losses of THz QCLs. This measurement technique allows access to the amplitude and phase spectra of the stimulated emission allowing the direct determination of the gain.[3,4] We apply the technique to a range of samples operating at different frequencies obtaining information on the subband alignment and the dominant transitions involved in the gain spectra. Further, as the technique is not sensitive to the laser emission of the QCL, the entire operating current range can be investigated, above as well as below laser threshold. (The phase of the emitted QCL radiation is not locked in time with respect to the femtosecond probe beam; therefore no electro-optic signal is detected from the QCL emission).

The set-up used to characterize the QCLs is based on a standard THz-TDS system in a transmission set-up. The devices under consideration with the THz-TDS system are AlGaAs/GaAs QCLs, based on bound-to-continuum optical transitions.[5] As the QCL is brought above laser threshold, a series of long lasting and strong oscillations are observed in the transmitted THz pulse (see Fig. 1), corresponding to an amplification of the broadband pulse over the gain of the QCL. Using a reference scan, the spectral gain of the laser emission can be determined.[4]

Figure 1a shows the time domain electric field of a transmitted THz-TDS pulse through a 2.1THz QCL. Oscillations of the electric field are observed, that are due to the amplification of the input pulse at the QCL gain. At the threshold current (J_{th}=89A/cm^2) the field oscillations die out quickly. However as the current density (and hence the bias field) is increased longer lasting oscillations are observed. At the laser shut-off current (136 A/cm^2), the field oscillations last almost twice as long as at threshold, indicating a reduction in the spectral width. The gain spectra of the 2.1THz device is shown in figure 1b, showing peak gain at 2.1THz i.e. at the emission frequency of the QCL. As the applied bias is increased the linewidth of the main peak at 2.1THz clearly decreases. Similar behaviour is observed in a 2.9THz laser.

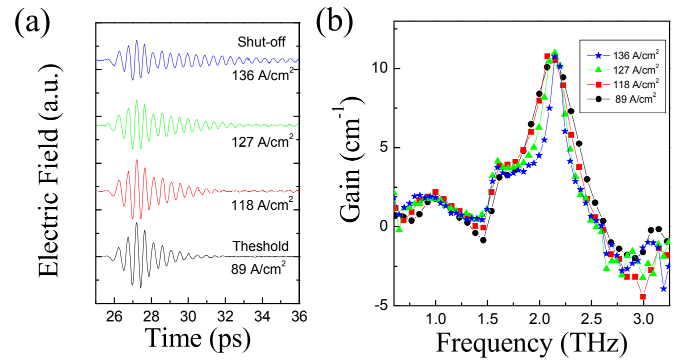

Fig. 1.a) Time domain electric fields of a THz pulse transmitted through a 2.1THz QCL as a function of applied current. b) Corresponding Fourier transformed spectra showing gain narrowing around 2.1THz above laser threshold.

Figure 2a shows the voltage-current density (V-J) and light output-current density (L-J) curves of the 2.1 THz laser. The power output of the QCL was measured using a pyroelectric detector. Below, figure 2b shows the gain at the laser frequency and the FWHM of the gain as a function of current density. Below threshold the gain of the laser increases sharply after 60A/cm^2 as the structure begins to align. The measured gain clamps near threshold (93 A/cm^2) at 11cm^{-1} due to laser action. (For the 2.9THz laser, the peak gain clamps at 7cm^{-1}). The gain remains constant until approximately 136A/cm^2 (where laser action ceases) after which it decreases rapidly.

The FWHM of the gain shows a continual reduction in the width as the current is increased to threshold where it stabilises to ~0.48THz for the 2.1THz QCL. Beyond this point the FWHM decreases at a much slower rate until the laser power saturates at 114A/cm^2. Surprisingly, after the point of maximum laser power is reached, the FWHM reduces sharply (the peak gain remains constant) with a minimum linewidth of 0.22THz at 136A/cm^2, after which laser action fully ceases.

978-1-4244-2120-6/08/$25.00 ©IEEE.

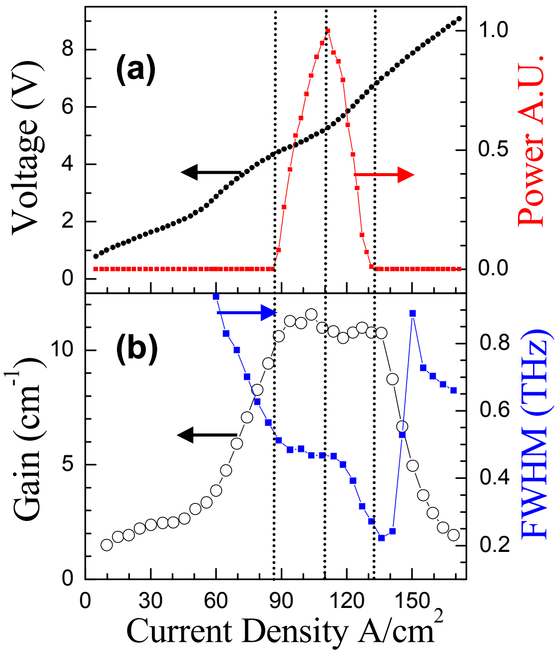

Fig. 2. a) V-J and L-J curves of the 2.1THz laser at 4.2K b) Spectral gain at the laser frequency, and FWHM of the gain as a function of current density at 4.2K. The vertical dashed lines correspond, from left to right, laser threshold, peak power output and laser shut-off.

We qualitatively explain these results in terms of the alignment and misalignment of the wavefunctions with applied bias. Figures 3a, b, and c show the bandstructure of the 2.1THz structure for bias fields of 1.5kV/cm, 1.9kV/cm, and 2.3kV/cm respectively, along with their corresponding moduli squared wave functions. The upper laser states (labeled L1, L2, and L) are red, and the miniband states are blue. The active region is indicated by the horizontal arrows in figure 3a, b, and c. The injector miniband states are coupled to the upper laser state via a 50nm injector well – the pink shadded region in figure 4a, b, c. The injector state in green (labeled i in figure 4 a,b,c) is mainly confined to this 50nm injector well.

As the field is increased from 1.5kV/cm (figure 3a) the injector miniband is shifted to higher energies with respect to the upper laser states. For some bias, the laser state will be aligned with the lowest energy state of the injector miniband (the injector state). In figure 3b at a bias field of 1.9kV/cm, the laser state is coupled to the injector state.[17] Indeed it is difficult to distinguish between the injector and laser states in figure 3b. The high coupling between the laser and injector states corresponds to resonant current injection[18] into the upper laser level and the maximium emitted power from the QCL. For larger bias fields, the injector miniband moves above the upper laser state. This results in a misalignment of the structure, a decrease in the injection efficiency, and hence a drop in the emitted QCL power. This is shown in figure 4c for a field of 2.3kV/cm, where the laser state is below the injector state, and the injector and laser states have become uncoupled. Thus for bias fields higher then the optimal injection (i.e. maximum power), shown in figure 3b, a *single* upper laser state contributes to the gain.

The observed narrowing of the spectral gain width after maximum power is therefore attributed to the formation of *single* upper laser level. This is in contrast to lower biases, where several highly coupled levels will contribute to the lasing transition. We will present results from other devices showing the gain and its evolution with applied field, its relation to the corresponding bandstructure and how this information can be applied to new QCL designs.

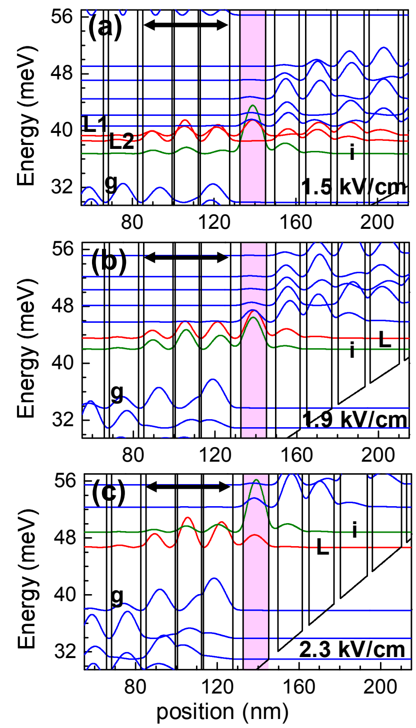

Fig. 3.a), b) and c) Square modulus of the wave functions, with the injector well (shaded pink) for biases of 1.5, 1.9 and 2.3kV/cm. The upper laser states (red) are labeled L1, L2 and L. The lower laser state is labeled g. The miniband states are in blue. The injector well state (labeled i) is in green.

REFERENCES

[1] R. Köhler, A. Tredicucci, F. Beltram, H. Beere, E. H. Linfield, A. G. Davies, D. A. Ritchie, R. C. Iotti, and F. Rossi, Nature **417**, 156 (2002).
[2] B. Williams, *Nature Photonics* **1**, 517 (2007).
[3] J. Kröll, J. Darmo, S. S. Dhillon, X. Marcadet, M. Calligaro, C. Sirtori and K. Unterrainer, *Nature* **449**, 698 (2007).
[4] N. Jukam, S. Dhillon, Z. Y. Zhao, G. Duerr, J. Armijo, N. Sirmons, S. Hameau, S. Barbieri, P. Filloux, C. Sirtori, X. Marcadet, and J. Tignon, *IEEE J. Selected topics in Quantum Electronics* **14**, March/April (2008).
[5] S. Barbieri, J. Alton, H. Beere, J. Fowler, E. Linfield, and D. A. Ritchie, *Appl. Phys. Lett.* **85**, 1674, (2004).